Computational and Spectroscopic Characterization of the Molecular and Electronic Structure of the Pb(II)−Quercetin Complex

J. P. Cornard,* L. Dangleterre, and C. Lapouge

LASIR, CNRS UMR 8516, Université des Sciences et Technologies de Lille, Bât C5-59655 Villeneuve d'Ascq Cedex, France

Received: June 28, 2005; In Final Form: September 9, 2005

The interactions of lead(II) ion with a polyhydroxylated flavonoid, the quercetin molecule, were investigated in methanol solution. The quercetin/metal stoichiometries and equilibrium stability constants for metal binding to quercetin have been determined by UV−vis spectroscopy combined with chemometrics methods. The 2:1, 1:2, and predominant 1:1 species are formed in solution. Among the three potential sites of chelation present in the quercetin structure, the catechol function presents the highest complexation power toward Pb(II), in opposition with previous results found for Al(III) complexation. This result has been confirmed by the good agreement of the experimental and theoretical features for both the electronic and vibrational spectra of the 1:1 complex. DT-DFT calculations show that the bathochromic shift of the long-wavelength band of the UV−vis spectra, that occurs upon complexation, is due to a ligand-to-metal charge transfer. The molecular structure of the ligand is not much modified by the coordination of lead at the level of the catecholate.

1. Introduction

Spectroscopic and analytical data have shown that humic acids of soils and sediments present several major functional groups, predominantly carboxylic and phenolic, as well as carbonyl and alcoholic functions.[1,2] These functions are known to significantly participate in the retention of pollutants as metals in natural environments. The transport, reactivity, bioavailability, and toxicity of metal ions are significantly affected by complexation reactions with the many potential sites of the macromolecules of humic acids. To gain a greater understanding of these reactions and of their mechanisms, it is useful to apply spectroscopic techniques combined with quantum chemical calculations to model compounds containing functional groups which are present in the polymeric substances. If a great number of papers[3−9] relate to the study of the metal complexation of small organic acids, used like model compounds of humic acids, few concern the polyphenolic functions which, however, play a considerable role in the chelation of metals. These reasons led us to compare the chelating capacity of acid and polyphenolic functions toward certain metals, like aluminum or lead,[10,11] but also to compare the polyphenolic functions themselves. In this respect, the flavonoid compounds, which form part of the polyphenols family, are molecules perfectly well adapted as models of a part of humic acids, insofar as these compounds are omnipresent in the vegetable kingdom and constitute precursors of the soil organic matter.[12−15]

Quercetin (3,3′,4′,5,7-pentahydroxyflavone) is one of the most common flavonols present in nature that has attracted the attention of many researchers because of its biological properties.[16−18] Quercetin possesses three possible chelating sites in competition: the 3-hydroxy-carbonyl, the 5-hydroxy-carbonyl, and the 3′,4′-dihydroxyl (catechol) functions (Figure 1). Complexation of metal cations by quercetin has already been reported for a great number of metals,[19−24] but almost no information is known on the lead(II)−quercetin system. Our preceding work[25] consisted in classifying, according to their power of complexation, the three potential sites of quercetin taken independently within three monosite ligands: 3-hydroxyflavone, 5-hydroxyflavone, and 3′,4′-dihydroxyflavone. One of the principal results of this study concerning the Pb(II)−hydroxyflavone systems showed that the three considered sites could be classified in the following way: catechol > α-hydroxy-carbonyl > β-hydroxy-carbonyl. The goals of this present work are (i) to determine the composition and the stability of the complexes obtained for the Pb(II)−quercetin system in methanol as well as the mechanism of complexation, (ii) to identify the predominant species and to achieve a structural analysis of this complex by quantum chemical calculations, and (iii) to check if the classification obtained with the monosite ligands remains valid when the various functions are in competition within the same multisite molecule.

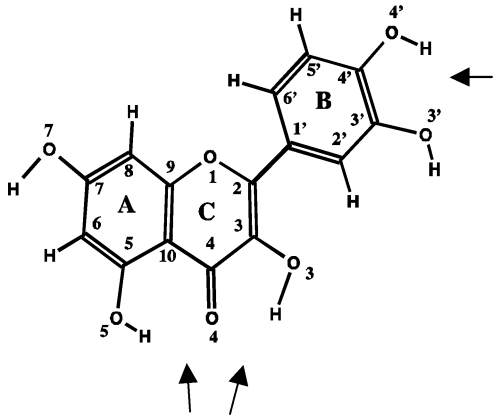

Figure 1. Representation and atomic numbering adopted for quercetin (IUPAC nomenclature). The arrows indicate the potential chelating sites.

2. Experimental Section

2.1. Reagents and Chemicals. The low solubility of flavonoids in water prevented us from working with the relatively

* Corresponding author. Phone: + 33-3.20.43.69.26. Fax: + 33-3.20.43.67.55. E-mail: cornard@univ-lille1.fr.

10.1021/jp053506i CCC: $30.25
Published on Web 10/19/2005

high concentrations necessary to obtain a Raman signal under good conditions; this is why methanol solutions were used. Quercetin was obtained from Extrasynthèse (France). Lead chloride and spectroscopic grade methanol were used without purification. The stoichiometries of the complexes were determined by the molar ratio method[26] from the UV−vis data set. For this method, solutions containing a constant concentration (4×10^{-5} M) of quercetin in methanol and variable concentrations of $PbCl_2$ (from 4×10^{-7} to 4×10^{-2} M) were prepared. The complexe's stoichiometry has also been verified by the method of continuous variation (Job's method).

The 1:1 complex was prepared by mixing, in methanol, adequate stoichiometric amounts of quercetin and lead chloride. Pale yellow precipitates were formed immediately when the cooled mixture was poured in water. The quercetin−complex mixture in crystalline form was then washed 3 times with 1:3 $EtOH/H_2O$, and several times with H_2O, and dried under vacuum.

2.2. Instrumentation. The UV−vis spectra were recorded on a Cary-l (Varian) spectrophotometer with cells of 1 cm path length, at 25 °C. A flow cell was used to allow successive additions of small amounts of lead(II) chloride directly in the flavonoid solution. FT-Raman spectra of quercetin and of its 1:1 complex with Pb(II) in methanoic solution (10^{-2} M) were recorded with a Bruker IFS 88W spectrometer connected to a Raman module (Bruker, FRA-106). An excitation in the near-infrared range (1064 nm from a Nd:YAG laser) has allowed the collection of free-fluorescence spectra. The Raman spectra of quercetin and of its 1:1 complex in the solid state were recorded with a Kaiser Raman microprobe (Hololab 5000). The laser (excitation: 785 nm) was focused on a single crystal in order to collect the Raman scattering of one or the other species in the quercetin−complex mixture.

2.3. Calculations. The absorption spectra collected during the course of the metal-binding experiment were analyzed with the fitting program SPECFIT (version 3.0).[27] This software allows the determination of the number of species that contribute to the absorption spectra using a factor analysis procedure (EFA)[28] and of the pure electronic spectrum of each complex. The Specfit software has also been used to estimate the stability constants (β) of the different complexed forms. To obtain the best fit between the complexation model and the experimental data, several models of complexes have been envisaged for the refinement of the stability constants.

The DFT calculations have been performed with the Gaussian 03 quantum chemical package[29] implemented on an IBM SP/Power 4 machine located at IDRIS (CNRS−France). Geometry optimizations of quercetin and its 1:1 complex with Pb(II) were obtained by using the three-parameters hybrid functional B3LYP.[30,31] The coordination of the Pb atom on each potential chelating site has been envisaged. For Pb, we adopted the Los Alamos double-ξ (Lanl2dz) and the 6-31G(d,p) basis set for the other atoms (including polarization functions, to correctly take into account intramolecular H-bondings present in the ligand). In our previous work, we have shown that the use of the quasi-relativistic Stuttgart/Dresden (MWB78) effective core potential for the description of the Pb atom has very little influence on the calculation of the electronic transitions observed in the complexes. For the free and complexed forms, harmonic vibrational frequency calculations have been performed to ensure that the optimized structures correspond to energy minima. Computed vibrational frequencies were scaled by a factor 0.97 for both the free ligand and the complex. This value corresponds to the average of the ratios of the experimental/calculated frequencies for each compound. Indeed, as scaling factors depend on the level of theory, the basis set, and the studied molecules,[32] we preferred to determine the best factor of our system than to use a predefined one.

The low-lying excited states were treated within the adiabatic approximation of time-dependent density functional theory (DFT-RPA)[33] with the B3LYP hybrid functional. Vertical excitation energies were computed for the first 40 singlet excited states, to reproduce the UV−vis spectra of the free and complexed quercetin. Solvent effects on calculated UV−vis spectra were introduced by the SCRF method, via the polarized continuum model (PCM)[34] implemented in the Gaussian program. In results, only transitions presenting high oscillator strengths (≥ 0.1) have been considered without focusing on their relative values, because it is well-known that, in such calculations, relative oscillator strengths are not reliable. Molecular orbitals involved in the main calculated electronic transitions have been drawn using the GaussView 3.09 program. One can note that the MOs calculated in vacuum and in methanol differ in energy but not in shape.

3. Results and Discussion

3.1. Stoichiometry of Complexes in Methanol. The electronic spectrum of free quercetin in methanol solution is mainly characterized by an important absorption band at 372 nm (band I) and a second one located at 255 nm (band II) with a shoulder at 269 nm (Figure 2a). Upon addition of lead(II) to the quercetin solution significant changes are observed in the electronic spectra. For [Pb(II)]/[Q] molar ratios less than 5, a new band toward high wavelengths (429 nm) is observed accompanied by an important decrease of the intensity of band I. At the same time, in the low-wavelength range, the band II intensity increases and a band located at 235 nm appears. The set of obtained spectra does not clearly show an isosbestic point, which would mean that several complexes are simultaneously formed. Further addition of the metal leads to the growth of the new band centered at 235 nm and a bathochromic shift of band I that reaches a maximum at 455 nm for a molar ratio of 15 (Figure 2b). This band seems to characterize a new absorbing species whose formation would start for a large amount of Pb(II) added.

The molar ratio method was used to determine the stoichiometry of the different complexed forms of quercetin with lead-(II). In this method ideally two straight lines are obtained when the absorbance at one wavelength is plotted versus the Pb(II) to flavonoid ratio, and the intersection point of these two lines corresponds to the stoichiometric ratio upon interpolation to the molar ratio axis. The molar ratio plots at 429 nm clearly indicate the formation of a complex of stoichiometry 1:1, whereas the plot at 455 nm shows two inflection points, for [Pb(II)]/[Q] = 0.5 and 2, corresponding to species of metal:ligand stoichiometry of 1:2 and 2:1, respectively. One can note that the application of the continual variations method (Job's method) to the dosage gives rise to the same results.

From the UV−vis absorption spectra, a finer determination of the number of different absorbing species was estimated by evolving factor analysis (Spectfit software). Four distinct components were found corresponding to the free quercetin and the three complexes with 1:2, 1:1, and 2:1 stoichiometry, previously calculated and temporarily noted PbL_2, PbL, and Pb_2L, respectively. To estimate the stability constants, a numerical treatment of the electronic spectra has been carried out with a model implicating the three complexes. The best-fitting model to the experimental data gives the following stability constants: $\log \beta = 7.71 \pm 0.43$, $\log \beta = 4.87 \pm 0.04$,

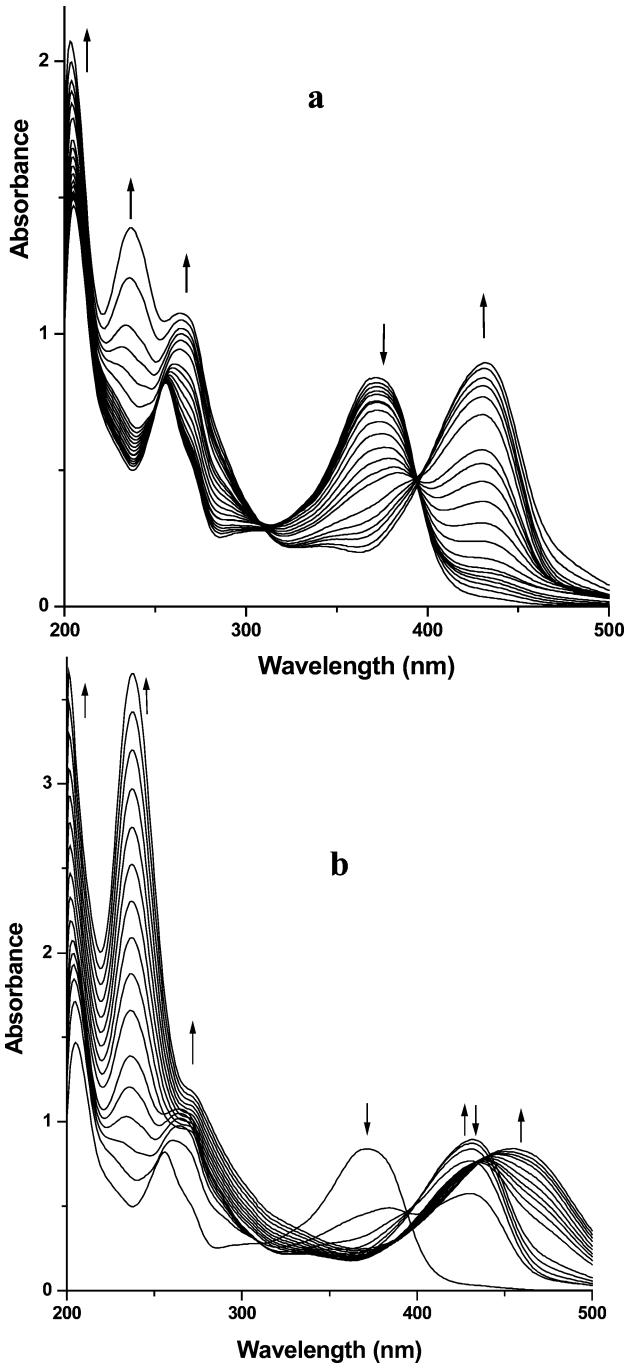

Figure 2. Electronic absorption spectra of quercetin in methanol in the absence and presence of $PbCl_2$ for molar ratios from 0 to 5 (a) and from 4 to 15 (b).

and $\log \beta = 8.23 \pm 0.05$ for PbL_2, PbL, and Pb_2L complexes, respectively. This result comes from the following reaction between lead and ligand (L):

$$a\mathrm{Pb} + b\mathrm{L} \leftrightarrow \mathrm{Pb}_a\mathrm{L}_b$$

with the corresponding stability constant:

$$\beta = \frac{[\mathrm{Pb}_a\mathrm{L}_b]}{[\mathrm{Pb}]^a[\mathrm{L}]^b}$$

Whatever the site implied in the complexation process, a deprotonation of the implicated hydroxyl groups occurs to allow the coordination of Pb(II).[35] However, this deprotonation at the level of the chelating site has not been taken into account in the constant calculation insofar as the pH notion has not much sense in a methanol medium. The concentration variations of the different species versus the quantity of lead added are illustrated in Figure 3a for values of the molar ratio ranging between 0 and 5, whereas Figure 3b represents an enlargment of the weak concentrations zone making it possible to observe the minority species. From the curves, it appears obvious that the predominant species is the 1:1 complex whose concentration is close to 75% for a molar ratio of 2. The PbL_2 species is formed from the beginning of the dosage, but remains very strongly a minority, since its concentration is always lower than 1%. The formation of the binuclear species is not immediate; one can estimate that the 2:1 complex starts to be formed for a molar ratio higher than 0.2, and its concentration reaches 1% for a ratio of 0.75. Thus, for example, for a molar ratio of 1 (4×10^{-4} M lead added) the various species are distributed in the following way expressed as a percentage: 0.6, 2.3, 54.9, and 42.2% for PbL_2, Pb_2L, PbL, and the free ligand, respectively, while the concentration of free Pb(II) in solution is about 1.7×10^{-5} M.

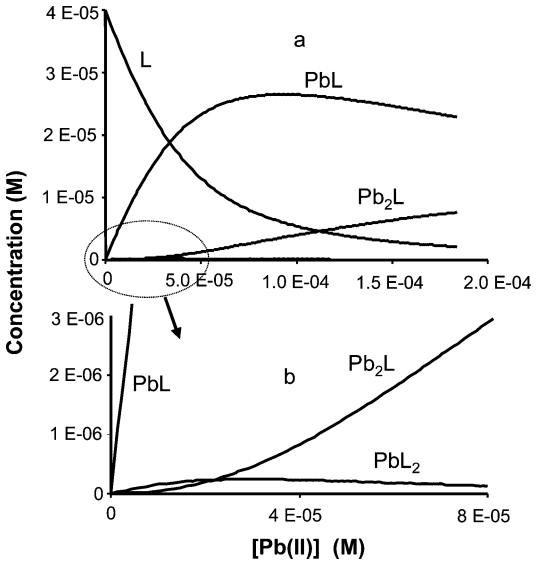

Figure 3. Distribution curves of free and complexed quercetin as a function of lead(II) concentration for [Pb(II)]/[Q] ratios between 0 and 5 (a) and between 0 and 2 (b).

From these observations, it is possible to propose the following mechanism: in a first step, the metal ion coordinates on a preferential site and leads to simultaneous formation of two complexes of stoichiometry 1:2 and 1:1; then, the complexation of a second site of quercetin (formation of the Pb_2L complex) largely starts before the complexation of the first site is completed. That means that the chelating powers of the two involved sites are close together in this molecule. However, it should be noted that the second site is involved for relatively high concentrations of Pb ions, much higher than one can find in natural environment. Zhou et al have reported that Pb^{2+} forms a complex with quercetin having a 1:2 metal/ligand ratio, with a coordination of the metal cation on the 3-hydroxy-carbonyl group;[36] but their experiment has been performed in ethanol solution in alkaline medium, with a single metal/ligand ratio of 0.5, and cannot be compared to our results taking into account the medium used. In the literature, coordination of various metals with only the 3-hydroxy-carbonyl and catechol sites are reported; the 5-hydroxy-carbonyl function of quercetin never seems to be involved in a process of complexation.[37] The complexation of lead(II) by quercetin caused in the UV−vis spectrum a bathochromic shift of 57 nm of band I for the first complex.

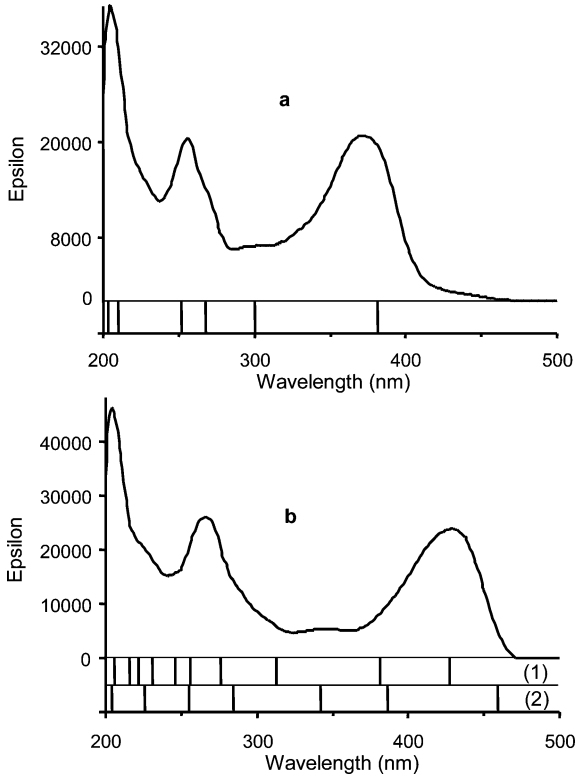

Figure 4. UV-vis spectra of quercetin (a) and its 1:1 complex (b) in methanol and positions of calculated electronic transitions (spectrum 1, with Pb^{2+} coordinated to the catechol site; spectrum 2, with Pb^{2+}-coordinated to the 3-hydroxy-carbonyl site).

This spectral shift is of the same order of magnitude as those observed for the complexation of Pb(II) by 3-hydroxyflavone (61 nm) and of 3′,4′-dihydroxyflavone (57 nm), whereas 5-hydroxyflavone presented a completely different behavior in the presence of lead with very similar electronic spectra for the free and complexed ligand.[25] These various arguments led us to think that only the 3-hydroxy-carbonyl or catechol functions are likely to be implied in the formation of the 1:1 complex. In the continuation of this paper, we will focus our attention only on the complex of 1:1 stoichiometry, which is the largely predominant species for a relatively small amount of lead present in solution.

3.2. Theoretical Electronic Absorption Spectra of Quercetin and Its 1:1 Complex. Quantum chemical calculations were carried out in order to achieve information about the first site involved in the chelation process of Pb(II) to form the PbL complex. The geometry optimizations of quercetin (Q), PbQ, and PbQ^+ with, respectively, the coordination of Pb(II) on the catechol and 3-hydroxychromone part, have been achieved at the DFT level of theory. From the most stable structure of each of these compounds, the theoretical electronic spectra have been calculated by a TD-DFT treatment, taking into account the solvent effect, at the B3LYP/6-31G(d,p) level. The Lanl2dz effective core potential was used for the description of the Pb atom for the two complexed forms. The experimental and calculated (vertical lines) UV−vis spectra of quercetin are represented in Figure 4a. The theoretical spectrum fairly well reproduces the shape of the experimental one. Even if only the transitions with an oscillator strength higher than 0.1 are taken into account, all the spectral features can be depicted by vertical transitions. However, the transition in the long wavelengths (381 nm) is calculated 9 nm higher than the observed band (372 nm). The experimental electronic spectrum of the PbL complex, directly obtained by singular value decomposition (Specfit), is reported in Figure 4b. Under this spectrum are represented the transitions calculated for both PbQ (1) and PbQ^+ (2) by taking into account the methanol effect. The great number of calculated transitions in both cases makes it possible to describe the UV−vis spectrum of PbL. But important differences are observed in the high-wavelength range in the two theoretical spectra and, notably, for the highest calculated transition. This last transition is calculated at 427 and 459 nm with a coordination of Pb(II) on the catecholate and on the 3-hydroxy-carbonyl function, respectively, whereas the absorption band is observed at $\lambda_{max} = 429$ nm. A difference of 30 nm between the experimental and the calculated spectrum with a chelation on the 3-hydroxy-chromone part tends to show that one can exclude this possibility. All the more that our previous works[38] have shown a very good accordance between the experimental and theoretical spectra of Pb(II)−monosite hydroxyflavone systems, validating the calculation method, the basis sets choice, and the fact that the solvent effect must be taken into account. Indeed, very small differences in wavelengths have been obtained between the calculated HOMO → LUMO transition and the experimental absorption band of the 1:1 complexes of 3-hydroxyflavone and 3′,4′-dihydroxyflavone (6 and 1 nm, respectively), using the same calculation methodology. So the transition calculated at 427 nm for PbQ, involving a contribution of 85% of HOMO → LUMO, reproduces very well the long-wavelength absorption band observed in the PbL solution spectrum (429 nm) and leads us to propose a chelation of Pb(II) on the catecholate function for the 1:1 complex.

Table 1 collects the wavelengths of the experimental spectra and of the calculated transitions of both free quercetin and its 1:1 complex with a lead coordination on the catecholate. Only the contribution of the transitions having an oscillator strength higher than 0.1 are reported; a great number of other transitions presenting much weaker probability could be added to these latter. The theoretical spectrum of PbQ presents numerous transitions, notably in the UV spectral range, which allows describing all the shoulders observed in the complex absorption spectrum. One can notice that the shape of the long-wavelength absorption band, which presents a bathochromic shift upon complexation, is not symmetric. For both the free and complexed quercetin, this band is assigned mainly to the HOMO → LUMO transition. The shoulder appearing in the low wavelengths could be assigned to a transition calculated at 381 nm, involving the HOMO → LUMO + 1 (contribution: 84%) in the complex, whereas it corresponds to the HOMO − 1 → LUMO transition, not represented in the figure because of its low calculated oscillator strength (0.03), in quercetin.

3.3. Frontier Orbitals Analysis. The frontier orbitals, and their energy, of quercetin and of its complex calculated in methanol are represented in Figure 5. The charge density for the HOMO of quercetin is mainly localized on the B ring and the C_2-C_3 bond, whereas the LUMO presents a charge density more distributed on the whole molecule, with a bonding character on the inter-ring bond. The HOMO → LUMO transition consists of a low charge transfer from the B ring to the A ring through the γ-pyrone part. The HOMO − 1 → LUMO transition in quercetin presents a charge redistribution toward the $C_4{=}O_4$ function. The HOMO and LUMO of the complex present exactly the same charge distributions on the ligand as that observed for the corresponding molecular orbitals of quercetin. They also, respectively, involve a very low and a very large participation of the 6p atomic orbital of the Pb(II) ion. So, the HOMO → LUMO transition in PbQ consists at the

TABLE 1: Experimental and Calculated (in Methanol) Wavelengths (nm) for Quercetin and Its 1:1 Complex with a Coordination on the Catechol Site[a]

quercetin			1:1 complex with Pb(II) on catecholate		
λ_{exptl} (nm)	λ_{calc} (nm)	MO contribution (%)	λ_{exptl} (nm)	λ_{calc} (nm)	MO contribution (%)
372	381	H → L (82)	429	427	H → L (85)
299	300	H-2 → L (89)	sh	381	H → L + 1 (84)
270 (sh)	268	H → L + 1 (44), H-3 → L (25)	sh	313	H-2 → L (81)
254	252	H-1 → L + 1 (54), H → L + 2 (15)	264	276	H-3 → L (42), H → L + 2 (36)
sh	211	H-1 → L + 3 (41), H-6 → L (29)	264	256	H → L + 4 (50), H-1 → L + 2 (27)
204	203	H-4 → L + 1 (22), H-3 → L + 3 (18), H-6 → L (10)	sh	247	H → L + 4 (35), H-1 → L + 2 (21), H → L + 5 (17)
			sh	231	H-2 → L + 2 (68)
			224	222	H-1 → L + 4 (50), H-3 → L + 2 (33)
			sh	216	H-1 → L + 5 (68)
			203	206	H-4 → L + 2 (34), H-3 → L + 4 (19)

[a] Only transitions with an oscillator strength >0.1 and molecular orbitals with a contribution >10% are reported.

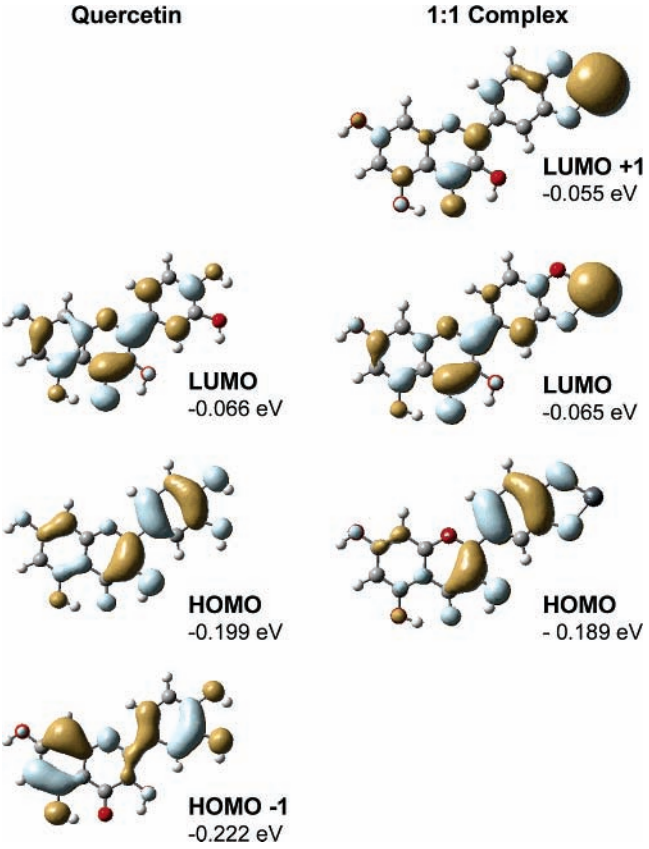

Figure 5. Plots of the frontier orbitals involved in the electronic transitions calculated for band I of quercetin and its 1:1 complex. The energy of each MO is given in eV.

same time in a low charge transfer from the B ring to the A ring through the γ-pyrone part and in important ligand-to-metal charge transfer which would be at the origin of the bathochromic effect observed in the spectrum upon complexation. The HOMO + 1 of the complex also presents a strong participation of the 6p orbital of lead, and consequently the HOMO → LUMO + 1 transition corresponds to a ligand-to-metal charge transfer.

3.4. Structural Analysis. The DFT calculations at the B3LYP/6-31G(d,p) level lead to a totally planar structure of the quercetin molecule, both in vacuum and with solvent effect. Indeed, a weak interaction between the O_3 and $H_{2'}$ atoms constrains the B ring to remain in the plane of the chromone part. This effect was already highlighted for 3-hydroxyflavone.[38] Among the different possibilities of the B ring orientation, the structure with a dihedral angle $O_1C_2C_{1'}C_{6'} = 0°$ is found the most stable. The geometry presenting an angle $O_1C_2C_{1'}C_{6'} =$ 180 ° lies 0.53 kcal mol^{-1} above the lowest energy one. Similar results have already been obtained by Leopoldini et al. using the B3LYP/6-311++G** level of theory[39] and a comparable energy difference between the two conformers. The comparison of structural parameters calculated with the 6-31G(d,p) and 6-311++G** basis sets are perfectly identical; this shows that the introduction of diffuse orbitals in the basis set does not improve the description of this molecular system. In opposition, calculations performed with the CHIH-DFT model with the 6-31G†† basis set give rise to a lowest energy structure with a $O_1C_2C_{1'}C_{6'}$ torsional angle of 180°.[40,41] Upon complexation, the ligand remains totally planar, and the lead atom coordinated to the catecholate group is in the same plane as quercetin. Table 2 reports the bond lengths of both quercetin and its complex. The data of this table clearly state that the complexation on the

TABLE 2: Bond Lengths (Å) Calculated for Quercetin and Its 1:1 Complex with Pb^{2+}

	quercetin	PbQ
O_1C_2	1.376	1.377
C_2C_3	1.371	1.373
C_3C_4	1.450	1.450
C_4C_{10}	1.432	1.433
$C_{10}C_5$	1.424	1.424
C_5C_6	1.391	1.391
C_6C_7	1.405	1.405
C_7C_8	1.398	1.398
C_8C_9	1.390	1.391
C_9C_{10}	1.408	1.407
C_9O_1	1.360	1.359
$C_2C_{1'}$	1.463	1.464
$C_{1'}C_{2'}$	1.413	1.408
$C_{2'}C_{3'}$	1.384	1.395
$C_{3'}C_{4'}$	1.407	1.421
$C_{4'}C_{5'}$	1.393	1.402
$C_{5'}C_{6'}$	1.391	1.386
$C_{6'}C_{1'}$	1.408	1.417
C_4O_4	1.263	1.264
C_3O_3	1.359	1.356
O_3H_3	0.981	0.981
C_5O_5	1.340	1.340
O_5H_5	0.992	0.993
$C_{3'}O_{3'}$	1.376	1.349
$O_{3'}H_{3'}$	0.965	
$C_{4'}O_{4'}$	1.357	1.342
$O_{4'}H_{4'}$	0.970	
C_7O_7	1.359	1.359
O_7H_7	0.967	0.967
$O_{3'}Pb$		2.068
$O_{4'}Pb$		2.081
$O_4\cdots H_5$	1.746	1.734
$O_4\cdots H_3$	1.976	1.982
$O_3\cdots H_{2'}$	2.141	2.162
$O_{3'}\cdots H_{4'}$	2.122	

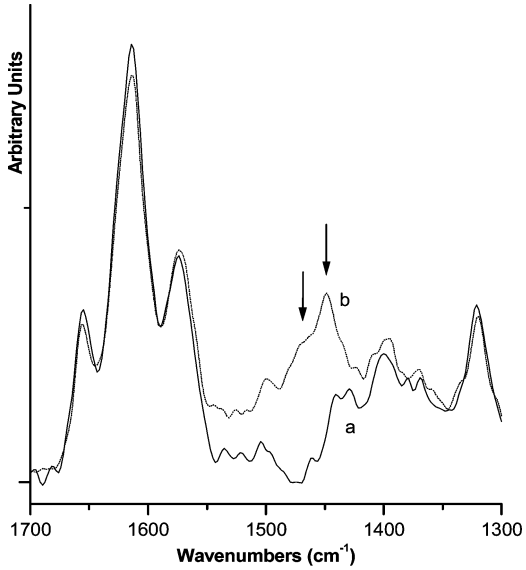

Figure 6. FT-Raman spectra of a solution of 10^{-3} M quercetin (a) and a mixture of 10^{-3} M quercetin and 5×10^{-4} M lead chloride (b), in methanol.

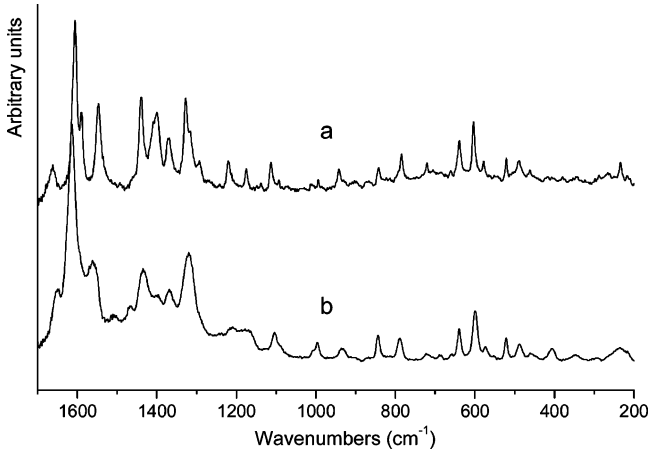

Figure 7. Raman spectra of a crystal of quercetin (a) and of a crystal of PbQ (b) recorded under a microscope.

catechol site not at all affects the structural parameters of A and C rings and does not modify the inter-ring bond length. On the other hand, the B ring undergoes light geometrical modifications. One can note a weak increase of the $C_{2'}C_{3'}$, $C_{3'}C_{4'}$, and $C_{4'}C_{5'}$ bond lengths accompanied by a very light decrease of the $C_{1'}C_{2'}$ and $C_{5'}C_{6'}$ bond lengths. In the same way, the bond angles of the B ring are slightly modified (results not shown) and undergo variations lower than 0.6°. At the chelating site level, a clear decrease of the bond lengths for $C_{3'}O_{3'}$ and $C_{4'}O_{4'}$ is calculated. However, the lengths of these two bonds are not identical and show a weak participation of a mesomeric cinnamoyl form on the B ring.[42] The lengths of two Pb−O bonds also differ from 0.013 Å. These results are in perfect agreement with those observed for 3′,4′-dihydroxyflavone, where only the B ring is affected by the metal chelation.[38] It should be noted that the results of the calculations show that a complexation of Pb(II) on the level of the 3-hydroxy-carbonyl site modifies in a very significant way the unit of the ligand structure.

3.5. Vibrational Analysis. Another confirmation of the coordination of Pb(II) on the catechol site is given by the subtle modifications of the Raman spectrum of quercetin in the presence of lead chloride in methanol. Figure 6 presents the FT-Raman spectrum of 10^{-3} M quercetin in methanol (spectrum a) and the FT-Raman spectrum of a mixture of quercetin and of its 1:1 complex in solution (spectrum b), in the range of 1300−1700 cm^{-1}. This mixture of the two forms has been obtained for a metal/ligand molar ratio of 0.5, where the 1:1 complexed form is largely predominant compared to the 1:2 and 2:1 species. However, for such ratio, a significant quantity of free ligand is still present in solution. One observes very few differences in the general shape of these two spectra. The band located at 1656 cm^{-1} and mainly assigned to the $C_4{=}O_4$ stretching mode does not shift in spectrum b; this band is calculated at 1656 cm^{-1} (scaled values) for both the free and the PbQ complexed form. The fact that the $C_4{=}O_4$ stretching does not move in frequency during the complexation confirms that the carbonyl function is not implied in the formation of the chelate. For the purpose of comparison, the $C_4{=}O_4$ stretching is calculated at 1647 cm^{-1} when the Pb atom is coordinated to the 3-hydroxy-carbonyl site. In the same way, the intense lines observed at 1614 and 1577 cm^{-1} and that at 1502 cm^{-1} are almost identical in the two spectra and can be assigned to the C_2C_3 stretching mode and the 8a and 8b modes of the A and B rings according to Wilson's notation.[43,44] These similarities are directly connected to the very weak structural modifications of the ligand engendered by the coordination of Pb(II) on the catecholate function. However, spectrum b reveals a relatively broad band in the 1400−1500 cm^{-1} spectral range, not observed in spectrum a, and in which one can raise two distinct lines at 1470 and 1447 cm^{-1} (marked by arrows). These new lines can be assigned to complex vibrational modes involving the $C_{4'}O_{4'}$

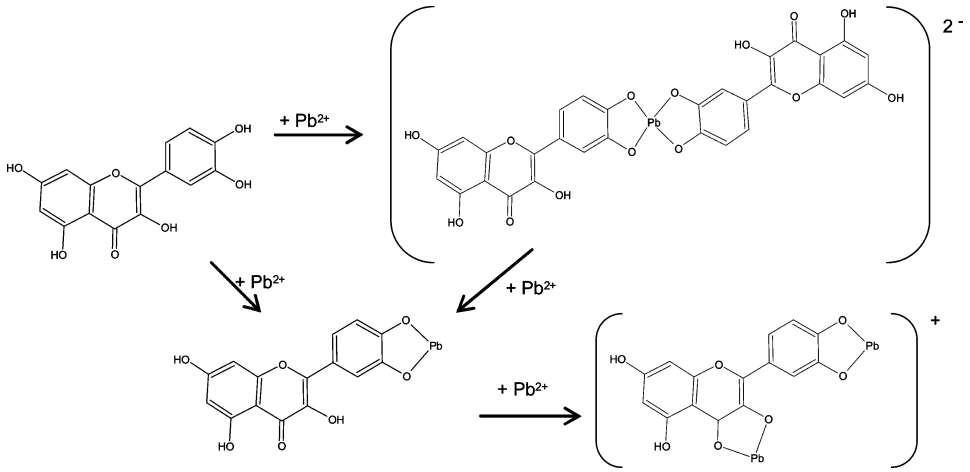

Figure 8. Proposed mechanism for the complexation of Pb(II) by quercetin.

and $C_{3'}O_{3'}$ stretching mechanically coupled to the 19a mode of the B ring. The asymmetric and symmetric Pb−O stretching modes, respectively, calculated at 398 and 287 cm^{-1}, could not be detected in the background noise of the Raman spectrum.

The mixture of quercetin and PbQ complex in methanol solution was then poured in a great quantity of water so as to precipitate the compounds. A yellow-colored mixture of crystals of quercetin and PbQ complex was thus obtained. The focalization of the laser on a single crystal under a microscope has allowed the recording of the micro-Raman spectrum either of quercetin or of the 1:1 complex in the solid state according to the selected crystal. The Raman spectrum of quercetin in the solid state (Figure 7a) differs considerably from that obtained in methanol solution, notably in the highest wavenumber range. These spectral changes are the results of various factors such as solvent effects and lattice interactions.[42] For instance, the $C_4{=}O_4$ stretching of quercetin, in the solid state, shifts to 1663 cm^{-1}, and the C_2C_3 stretching and 8 modes of the phenyl rings see their frequencies largely modified. In a way less marked than that for quercetin, the Raman spectrum of the complexed form (Figure 7b), recorded in the solid state, differs from that observed in solution. The $C_4{=}O_4$ stretching of the complex can be assigned to the line observed at 1652 cm^{-1}. This high value in frequencies shows once again that the carbonyl function is not implied in the coordination of lead in the 1:1 complex. Indeed, many examples in the literature show that whatever the nature of the metal, a complexation at the level of the 3-hydroxy-carbonyl site lowers the C=O stretching frequency in the 1637−1640 cm^{-1} range.[23,45,46] A line of low intensity appears at 406 cm^{-1} in the spectrum of the complex and can be assigned to the asymmetric Pb−O stretching modes.

4. Conclusion

The results of this study provide further information regarding the complexation of Pb(II) ions with quercetin, which can be considered as a model molecule of humic substances. Combined spectroscopic and theoretical approaches have allowed the comparison of the chelating power toward lead ion of the three potential sites present in quercetin. Among these three sites in competition, both electronic and vibrational spectroscopies have demonstrated that the catechol group presents the greater complexing power toward Pb(II). The most predominant complexed form obtained for a low amount of lead chloride is clearly the 1:1 complex, and the second chelating site, the 3-hydroxy-carbonyl group, is only involved for metal/quercetin ratios higher than 0.2. The different obtained results lead us to propose the mechanism of complexation illustrated in Figure 8. These results also show that the classification of the various sites taken individually (monosite hydroxyflavones) is preserved when these same sites are in competition within only one molecule (multisite hydroxyflavone). This last point is encouraging and illustrates the possibility to compare the chelating power toward a given metal of different groups in competition in a polyfunctional macromolecule by studying each group independently, in well-defined physicochemical conditions.

It is also interesting to note that the behavior of Pb(II) completely differs from the Al(III) one, which preferentially coordinates the 3-hydroxy-chromone part of quercetin.[42]

Finally, this contribution shows that the TD-DFT methodology can be easily applied to the electronic absorption spectra calculations of the Pb(II) complex, and the obtained results are in very good agreement with the experimental features if solvent effects are taken into account. Moreover, a complete assignment of the spectral changes observed upon complexation of such compounds can be deduced from these calculations.

Acknowledgment. "Institut du Développement et des Ressources en Informatique Scientifique" (IDRIS—Orsay, France) is thankfully acknowledged for the CPU time allocation. The authors also thank the Lille University Computational Center.

References and Notes

(1) Schulten, H. R. *Humic Subtances in the Global Environment and Implications on Human Health*; Senesi, N., Miano, T. M., Eds.; Elsevier: Amsterdam, 1994.

(2) Tipping, E. *Cation Binding by Humic Substances*; Cambridge University Press: Cambridge, U.K., 2002.

(3) Elkins, K. M.; Nelson, D. J. *Coord. Chem. Rev.* **2002**, *228*, 205.

(4) Borges, F.; Guimaraes, C.; Lima, L. F. C.; Pinto, I.; Reis, S. *Talanta* **2005**, *66*, 670.

(5) Plaschke, M.; Rothe, J.; Denecke, M. A.; Fanghänel, T. *J. Electron. Spectrosc. Relat. Phenom.* **2004**, *135*, 53.

(6) Giannakopoulos, E.; Christoforidis, K. C.; Tsipis, A.; Jerzykiewicz, M.; Deligiannakis, Y. *J. Phys. Chem. A* **2005**, *109*, 2223.

(7) Francioso, O.; Sanchez-Cortes, S.; Casarini, D.; Garcia-Ramos, J. V.; Ciavatta, C.; Gessa, C. *J. Mol. Struct.* **2002**, *609*, 137.

(8) Miano, T.; Sposito, G.; Martin, J. P. *Geoderma* **1990**, *47*, 349.

(9) Maria, P. C.; Gal, J. F.; Massi, L.; Burk, P.; Tammiku-Taul, J.; Tamp, S. *Rapid Commun. Mass. Spectrom.* **2005**, *19*, 568.

(10) Cornard, J. P.; Lapouge, C. *J. Phys. Chem. A* **2004**, *108*, 4470.

(11) Boilet, L.; Cornard, J. P.; Lapouge, C. *J. Phys. Chem. A* **2005**, *109*, 1952.

(12) Coulson, C. B.; Davies, R. I.; Lewis, D. A. J. *Soil Sci.* **1960**, *11*, 20.

(13) Remko, M.; Polcin, J. *Collect. Czech. Chem. Commun*. **1980**, *45*, 201.

(14) Smith, D. S.; Kramer, J. R. *Environ. Int.* **1999**, *25*, 295.

(15) Smith, D. S.; Kramer, J. R. *Anal. Chim. Acta* **2000**, *416*, 211.

(16) Leighton, T.; Ginther, C.; Fluss, L.; Harter, W.; Cansado, J.; Notario, V. *Phenolic Compounds in Foods and their Effects on Health II*; Huang, T., Ho, C. T., Lee, C. Y., Eds.; ACS Symposium Series 507; American Chemical Society: Washington, DC, 1992; p 220.

(17) Hollman, P.; Hertog, M.; Katan, M. *Food Chem.* **1996**, *57*, 43.

(18) Moreira, A. J.; Fraga, C.; Alonso, M.; Collado, P. S.; Zetller, C.; Marroni, C.; Marroni, N.; González-Gallego, J. *Biochem. Pharmacol.* **2004**, *68*, 1939.

(19) Torreggiani, A.; Tamba, M.; Trinchero, A.; Bonora, S. *J. Mol. Struct.* **2005**, *744−747*, 759.

(20) Le Nest, G.; Caille, O.; Woudstra, M.; Roche, S.; Guerlesquin, F.; Lexa, D. *Inorg. Chim. Acta* **2004**, *357*, 775.

(21) Katyal, M.; Prakash, S. *Talanta* **1977**, *24*, 367.

(22) Escandar, G. M.; Sala, L. F. *Can. J. Chem.* **1991**, *69*, 1994.

(23) Zhou, J.; Wang, L.; Wang, J.; Tang, N. *J. Inorg. Biochem.* **2001**, *83*, 41.

(24) Zhou, J.; Gong, G.; Zhang, Y.; Qu, J.; Wang, L.; Xu, J. *Anal. Chim. Acta* **1999**, *381*, 17.

(25) Dangleterre, L.; Cornard, J. P. *Polyhedron* **2005**, *24*, 1593.

(26) Yoe, J. H.; Jones, L. *Ind. Eng. Chem. Anal*. **1944**, *16*, 11.

(27) *Specfit Global Analysis System*, version 3.0; Spectrum Software Associates: Marlborough, MA.

(28) Gampp, H.; Maeder, M.; Meyer, C. J.; Zuberbühler, A. *Talanta* **1986**, *33*, 943.

(29) Frisch, M. J.; Trucks, G. W.; Schlegel, H. B.; Scuseria, G. E.; Robb, M. A.; Cheeseman, J. R.; Montgomery, J. A., Jr.; Vreven, T.; Kudin, K. N.; Burant, J. C.; Millam, J. M.; Iyengar, S. S.; Tomasi, J.; Barone, V.; Mennucci, B.; Cossi, M.; Scalmani, G.; Rega, N.; Petersson, G. A.; Nakatsuji, H.; Hada, M.; Ehara, M.; Toyota, K.; Fukuda, R.; Hasegawa, J.; Ishida, M.; Nakajima, T.; Honda, Y.; Kitao, O.; Nakai, H.; Klene, M.; Li, X.; Knox, J. E.; Hratchian, H. P.; Cross, J. B.; Adamo, C.; Jaramillo, J.; Gomperts, R.; Stratmann, R. E.; Yazyev, O.; Austin, A. J.; Cammi, R.; Pomelli, C.; Ochterski, J. W.; Ayala, P. Y.; Morokuma, K.; Voth, G. A.; Salvador, P.; Dannenberg, J. J.; Zakrzewski, V. G.; Dapprich, S.; Daniels, A. D.; Strain, M. C.; Farkas, O.; Malick, D. K.; Rabuck, A. D.; Raghavachari, K.; Foresman, J. B.; Ortiz, J. V.; Cui, Q.; Baboul, A. G.; Clifford, S.; Cioslowski, J.; Stefanov, B. B.; Liu, G.; Liashenko, A.; Piskorz, P.; Komaromi, I.; Martin, R. L.; Fox, D. J.; Keith, T.; Al-Laham, M. A.; Peng, C. Y.; Nanayakkara, A.; Challacombe, M.; Gill, P. M. W.; Johnson, B.; Chen, W.; Wong, M. W.; Gonzalez, C.; Pople, J. A. *Gaussian 03*, revision B.04; Gaussian, Inc.: Pittsburgh, PA, 2003.

(30) Becke, A. D. *J. Chem. Phys*. **1993**, *98*, 5648.

(31) Lee, C.; Yang, W.; Parr, R. G. *Phys. Rev. B* **1988**, *37*, 785.

(32) Scott, A. P.; Radom L. *J. Phys. Chem*. **1996**, *100*, 16513.

(33) Bauernschmitt, R.; Ahlrichs, R. *Chem. Phys.* **1996**, *256*, 454.

(34) Cossi, M.; Scalmani, G.; Rega, N.; Barone, V. *J. Chem. Phys.* **2002**, *117*, 43.

(35) Türkel, N.; Berker, M.; Özer, U. *Chem. Pharm. Bull.* **2004**, *52*, 929.

(36) Zhou, J.; Wang, L.; Wang, J.; Tang, N. *Transition Met. Chem.* **2001**, *26*, 57.

(37) Esparza, I.; Salinas, I.; Santamaria, C.; Garcia-Mina, J. M.; Fernandez, J. M. *Anal. Chim. Acta* **2005**, *543*, 267.

(38) Lapouge, C.; Cornard, J. P. *J. Phys. Chem. A* **2005**, *109*, 6752.

(39) Leopoldini, M.; Marino, T.; Russo, N.; Toscano, M. *Theor. Chem. Acc.* **2004**, *111*, 210.

(40) Mendoza-Wilson, A. M.; Glossman-Mitnik, D. *J. Mol. Struct. THEOCHEM* **2004**, *681*, 71.

(41) Mendoza-Wilson, A. M.; Glossman-Mitnik, D. *J. Mol. Struct. THEOCHEM* **2004**, *716*, 67.

(42) Cornard, J. P.; Merlin, J. C. *J. Inorg. Biochem.* **2002**, *92*, 19.

(43) Wilson, E. B. *Phys. Rev.* **1934**, *45*, 706.

(44) Varsanyi, G. *Assignment for Vibrational Spectra of Seven Hundreds Benzene Derivatives*; Lang, L., Ed.; Hilger: Budapest, 1974.

(45) Yuldashev, R. K.; Makhkamov, K. M.; Sharipov, K. T.; Aliev, K. U. *Chem. Nat. Compd.* **1999**, *35*, 420.

(46) De Souza, R. F. V.; De Giovani, W. F. *Spectrochim. Acta, Part A* **2005**, *61*, 1985.